



THE UNIVERSITY OF TENNESSEE

DEPARTMENT OF MECHANICAL
AND AEROSPACE ENGINEERING

GPO PRICE \$ _____

CFSTI PRICE(S) \$ _____

Hard copy (HC) _____

Microfiche (MF) _____

THEORETICAL AND EXPERIMENTAL STUDIES OF
VISCO TYPE AND BUFFERED SHAFT SEALS

ff 653 July 65

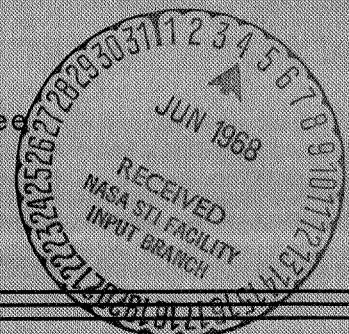
Semi-annual Progress Report
October 15, 1967-April 15, 1968

by

William K. Stair
Charles F. Fisher, Jr.
Edison A. Picklesimer, Jr.

May 1968

Knoxville, Tennessee



N 68-26843

(ACCESSION NUMBER) 32

(PAGES) 15

(THRU) _____

(CODE) 15

(CATEGORY) _____

(NASA CR OR TAX OR AD NUMBER) AL 9485

FACILITY FORM 602

The University of Tennessee
Department of Mechanical and Aerospace Engineering

THEORETICAL AND EXPERIMENTAL STUDIES OF
VISCO TYPE AND BUFFERED SHAFT SEALS

Semi-annual Progress Report
October 15, 1967-April 15, 1968

by

William K. Stair
Charles F. Fisher, Jr.
Edison A. Picklesimer, Jr.

Investigation conducted for the
National Aeronautics and Space Administration
under
Research Grant NsG-587

Reproduction in whole or in part is permitted
for any purpose of the U. S. Government

May 1968

Knoxville, Tennessee

ABSTRACT

This report, the eleventh of a series, outlines the progress made on the investigation of the viscoseal and the buffered seal during the period October 15, 1967 - April 15, 1968. The study is being conducted for The National Aeronautics and Space Administration under Research Grant NsG-587.

The experimental performance of four grooved-shaft seals is presented. These results, in addition to those for twenty three geometries previously reported, indicate that the theory advanced provides a good design estimate for grooved-shaft viscoseals in both laminar and turbulent regions. The performance of large diameter viscoseals having the same geometric parameters is relatively insensitive to the length of the land-groove pair when operated in the turbulent region.

The radial load carrying capacity of a viscoseal was found to be 12 to 15 percent of the capacity of a full journal bearing of the same overall dimensions.

Studies of interface stability has lead to a hypothesis for the mechanism of gas ingestion in viscoseals.

I. INTRODUCTION

An investigation embracing the theory and performance of the viscoseal under laminar and turbulent conditions was initiated on April 15, 1964 at The University of Tennessee in the Department of Mechanical and Aerospace Engineering. The investigation is being conducted for The National Aeronautics and Space Administration under Research Grant NsG-587, and this report presents the progress of the investigation for the period October 15, 1967 through April 15, 1968.

A critical review of all available literature led to the identification of a number of problem areas requiring study in support of the United States' space effort (1). Other reports in this series describe the program objectives (2), the design and construction of the experimental facility (3), the concentric laminar analysis of the viscoseal (4), the concentric turbulent analysis of the viscoseal (5), and results of experiments with the first twenty three viscoseal geometries (6,7,8,9). This report presents the experimental radial load capacity of a viscoseal, observations made on the gas ingestion study, and describes the buffered bushing seal program.

¹Numbers in parenthesis refer to similarly numbered references listed at the end of this report.

II. OBJECTIVES

The research program presented in references (2) and (3) was modified, as described in reference (6), because of the phenomenon of gas ingestion which was encountered during early experimental observations. In addition the scope of the research program was expanded to embrace the buffered bushing seal.

III. ACTIVITIES

Experimental work continued on the performance of the viscoseal and tests, described in a subsequent section of this report, were completed for four viscoseal geometries.

Tests on the first twenty two viscoseal geometries were made on the test facility described in reference (3). A modified test rig was prepared and utilized in testing viscoseal 6E. The results of the initial test on seal 6E showed considerable deviation between theory and experiment as noted in reference (9). The test rig was disassembled, checked, and reassembled. The repeat tests on seal 6E showed considerable improvement in agreement between theory and experiment.

The study of interface stability and gas ingestion continued. The test facility described in reference (9) was used to make still and high-speed moving picture studies of gas ingestion in plain and grooved annuli using a variety of test fluids. From these studies a new hypothesis for the mechanism of gas ingestion was evolved. In

addition to the gas ingestion studies the interface stability facility was used in making performance tests of three large diameter viscoseals.

The first series of experiments on the radial bearing load capacity of a viscoseal was completed. These tests indicate that the radial bearing capacity of a typical viscoseal geometry is about 12 to 15 percent of the capacity of a plain bearing having the same overall dimensions. Two new studies of the radial load capacity were initiated.

Analytical study of the turbulent buffered bushing seal continued. The design of the buffered seal test facility was completed and shop fabrication was started.

Mr. T. A. Arehart, Jr. completed his project assignment in January 1968 and is engaged in writing his thesis. The effort to obtain additional graduate research assistants continued throughout this period. While this is becoming an increasingly difficult problem, we have been able to make an appointment to Mr. Larry Luttrull who will undertake a project research assignment in June 1968.

IV. EXPERIMENTAL RESULTS

The test rig described in reference (3) was used in the tests for the first twenty two viscoseal geometries. The modified test rig shown in reference (9) was used to test seal 6E. Due to rather large experimental errors noted in the initial tests of seal 6E, a complete check was made of

the test rig, instrument calibrations, and the data reduction program. The repeated test on seal 6E is shown in Figure 1 in comparison with the initial test and with the tests for seals 6 and 6D which had similar geometric parameters. The error was apparently caused by the thermocouple circuit of the new test rig. Test work is under way on grooved housing seals 3H and 6H.

Performance tests were also made on three large diameter viscoseals. These seals, which were also used in connection with air ingestion studies in the interface stability test facility, have dimensions and geometric parameters shown in Table 1. The seals were

Table 1

DIMENSIONS AND GEOMETRIC PARAMETERS OF TEST SEALS

Seal No.	n	D	c	h	a'	b'	α	β	γ
11	3	3.990	0.006	0.045	0.524	0.524	14.5	8.5	0.5
12	6	3.990	0.006	0.045	0.262	0.262	14.5	8.5	0.5
13	12	3.990	0.006	0.045	0.131	0.131	14.5	8.5	0.5

D = seal diameter, in.; c = radial clearance, in.; h = groove depth, in.; α = helix angle, deg.; $\beta = (h+c)/c$; $\gamma = b'/(a'+b')$; a' = land width, in.; b' = groove width, in.

a' and b' dimensions are measured normal to groove.

installed in the interface stability test rig and arranged as shown in Figure 2. The Δp was measured by a mercury manometer connected to taps number 2 and 4 for which the center-to-center

distance was measured to be 2.01". The temperature in the fluid film was measured by a copper-constantan thermocouple inserted through tap location 3. The test fluid was distilled water and the annulus was filled to within 0.25" to 0.75" of the top of the test journal. The unused pressure taps were plugged to prevent ingress of air and the manometer lines could be easily bled of entrapped air. While test speeds could be reached at which air ingestion was evident for each test seal, the data were taken under conditions where the lower half of the annulus was free of air. When air ingestion was moderate to severe the seal could be run only for a finite length of time before enough air became trapped to blow the fluid out of the annulus. In these situations the seal cavity was drained, refilled, and started at a predetermined speed and the data recorded in a period of 60 to 90 seconds.

The large diameter seal tests are being made primarily to observe the effect of the characteristic length L^* on the onset of turbulence in a viscoseal. In the theoretical analysis presented in reference (5), which neglects inertia effects, the initiation of turbulence was taken to be at a critical Reynolds number defined as:

$$Re_{crit} = 41.1 \left[\frac{D/2}{(1-\gamma)c + \gamma\beta c} \right]^{1/2} . \quad (1)$$

A later analysis (10) shows that the relative magnitude of the convective inertia forces and viscous forces may be indicated by employing a modified Reynolds number, Re^* , defined as:

$$Re^* = Re_c(c/L^*); \text{ if } (c/L^*) < 1. \quad (2)$$

$$\text{where: } Re_c = \frac{Uc \rho}{\mu}$$

L^* = characteristic length

This analysis concludes that the inertia effects can be neglected only when $Re^* \leq 0.01$ and that these effects become significant in improving the sealing coefficient when $Re^* \approx 1$. In the case of the viscoseal L^* is taken as the length of the land-groove pair in the direction of motion. Thus,

$$Re^* = Re_c \left(\frac{cn}{\pi D} \right). \quad (3)$$

where: n = number of thread starts

As shown in Table 1 seals 11,12, and 13 have the same D , c , h , α , β , and γ but have differing L^* values. Figure 3 presents the experimental results obtained for these seals in comparison with the theoretical performance. The solid line in Figure 3 represents the predicted performance based on the analysis in reference (5) which gives the same curve for the three seals. The dashed lines represent the predicted performance considering the ideas suggested

in reference (10). The dashed lines were drawn by assuming that the transition would begin at $Re^* = 1$ and that the general shape of the curves in the turbulent region would be similar. On this basis the Re_c values at which transition would start are 700, 350, and 175 respectively for 3, 6, and 12 thread starts. From Figure 3 it will be noted that these preliminary experimental data show only fair agreement with theory and are not extensive enough to show the transition points. These data do, however, indicate that in the Re_c range of 1000 to 6000 the performance, in the absence of entrained gas, is essentially the same for all three seals.

It must be emphasized that these tests were made with negligible amounts of entrained gas as noted from a visual examination. These three seals would not function equally well in long term operation in the test facility. Seal No. 11 could be operated continuously at Re_c values of 3000-3500 without appreciable gas ingestion and tests at the highest speeds with Re_c of 5700 could be operated for extended periods before the gas accumulation became large enough to cause difficulty.

In the case of seal No. 12 gas ingestion became significant at a Re_c of approximately 2000 but ample time was available (5 to 10 minutes) to make observations at Re_c values in excess of 6000. It appeared that seal No. 12 could be operated for extended periods at Re_c values of

1500-2000.

Seal No. 13 was much more susceptible to gas ingestion which became noticable at Re_c values of 500-600 and severe at Re_c values of 1500-1800. At higher speeds it was necessary to make the test runs of short duration. At 3950 rpm ($Re_c \approx 4600$), for example, the air accumulation in a two minute period would be sufficient to force the liquid out of the annulus.

Additional experimental work scheduled for the large diameter seals includes:

1. Performance with glycerol-water mixtures to extend the range to lower Re_c values.
2. Tests with a back-flow of test fluid to sweep out ingested air.
3. Comparison of high and low frequency response instrumentation for determining pressure gradients in the seal.

Interface stability and gas ingestion studies described in reference (9) have continued. Experimental observation techniques employed were visual examination, single exposure photographs with 1.2 micro-second exposure times, and high-speed motion pictures with exposure rates from 1000 to 5000 pictures per second.

An annulus of 0.0105 inches thickness, using a plain aluminum cylinder having a diameter of 3.981 inches and a runout of 0.0003 inches was operated when approximately

two thirds filled with water. Air bubbles were observed at 900 rpm ($Re_c = 1250$) and the bubbles were observed to be aligned in circumferential rows when the shaft speed was above 2900 rpm, corresponding to $Re_c = 4000$ and Taylor number = 294. These rows were attributed to the presence of Taylor vortices as noted in Reference (9).

While working with this annulus, an interesting event was observed when, inadvertently, bands of liquid and bands of air were formed in the annulus as water was being introduced into the space under the cylinder while the shaft was turning at about 500 rpm and tilted at an angle to the vertical. These circumferential bands were generally about 0.05 inches in width and it was determined from a photograph that about fifty such bands of liquid were present. With the shaft turning at 950 rpm the pressure was changed to displace the bands and it was found that an estimated pressure change of two psi was required to cause these bands to move in either direction. After the shaft was stopped the bands appeared to maintain their shape for at least three minutes, after which time a photograph was taken. This photograph was so similar to those made while the shaft was turning that there appears to be no way to distinguish between them. Next, the pressure under the cylinder was changed to displace the bands axially and it was found that a pressure change of nearly two psi was required to initiate the displacement.

No effort was made to duplicate these events, and no significant effort has been made to determine the mechanics of the observed phenomena. The shaft speed of 950 rpm corresponds to $Re_c = 1325$ (transitional region) and a Taylor number of 96 compared to a critical number of 41.2 for beginning of Taylor vortices. No speculation is offered as to whether or not there is any connection between these numbers and the observed physical phenomena. Neither is it known if the same physical factors were responsible for the events observed in the dynamic case and the static case. For the static case, one can calculate the force per inch of interface line of contact on the solid surfaces and find that it is about the same as the value for a drop of water clinging to a vertical plane. However, it would seem presumptuous to extend this explanation to the case of the rotating shaft without further study.

With a plain aluminum cylinder, having a diameter of 3.990 inches, installed inside the acrylic cylinder with an inside diameter of 4.002 inches, high speed movies were made of the air-water interface. When the shaft speed was 1280 rpm ($Re_c = 1015$, Taylor number = 55.7) a breakup of the interface was observed to occur over approximately one third of the circumference. The interface level at any given circumferential location on the acrylic cylinder fluctuated approximately 3/16" because of runout. The break in the interface was observed to begin when the cylinder

had rotated 60 to 75 degrees after the maximum interface level had been attained. At 900 rpm the same region of the interface was observed to have a wavy or saw-tooth shaped profile with local height variations of about 0.02 to 0.03 inches. At this lower speed no air was seen trapped below the interface.

The region in which the waves, or interface break, occur is one in which the interface velocity is in the direction of the liquid, which for this case was the more viscous fluid. Somewhat analogous to this physical situation is the case of the motion of an interface separating two fluids between two closely spaced parallel planes which have no relative motion. A stability analysis of such an interface is presented by Saffman and Taylor (11) where it is shown that in the absence of gravity and surface tension the interface is unstable when the velocity is toward the more viscous fluid and stable when the velocity is in the opposite direction. When the gravitational force is taken into account (for vertical orientation of the planes) it is shown that there is a critical interface velocity which separates stable from unstable conditions. Further, it is shown that the effect of surface tension is to limit the range of unstable disturbances to those having a wavelength greater than a critical value, which is proportional to the square root of the surface tension.

Closely related to this is an analysis presented by Taylor (12) and experimentally verified by Lewis (13) showing that when two superposed fluids of different densities and negligible viscosities are accelerated in a direction perpendicular to their interface, this surface is stable or unstable for small deviations according as the acceleration is directed from the more dense to the less dense fluid or vice versa.

The instabilities referred to above lead to finite disturbances in the form of fingers of one fluid penetrating into the other, as sketched in Figure 4. Similar fingers have frequently been seen in the surface tension study facility, when the shaft was not rotating, as the interface level was being lowered.

In the case of an annulus with relative motion between the cylindrical surfaces, any eccentricity or runout causes the interface level to undergo periodic fluctuations. It seems highly probable that in this case an unstable perturbation would also occur for some range of conditions. With finite growth of the perturbations until fingers of gas protrude into the liquid, it then seems likely that some of the fingers would neck down and isolate a quantity of air (a bubble) from the interface, as shown in Figure 5. While this seems feasible, it must be regarded as an hypothesis, although some of our observations support the logic of this reasoning. Such fingers have been seen to develop

when the shaft was rotating at about 100 rpm or less, the fingers developing in a region where the interface level was descending and then the fingers withdrawing in a region where the interface level was rising. However, no air bubbles were seen to become trapped at a significant distance below the interface at the time of our observations.

At higher shaft rotational speeds, particularly when fluids of very low viscosity are used, the acceleration effects may dominate in leading to interface instability. This mechanism would probably become more important as the distance between the solid surfaces is increased. If so, this could mean that an interface between two surfaces having relative motion and a varying distance separating the surfaces, as in a viscoseal or a spiral grooved face seal, could have both types of instability occurring simultaneously.

Three viscoseal shafts shown in reference (9), Figure 4 were tested during this period and high speed movies were made to facilitate studies of the interface and the motion of air bubbles. The viscoseal shafts were made of aluminum with dimensions as shown in Table 1. An acrylic housing was used.

Movie film of the three thread-start shaft operating at 380 rpm ($Re_c = 300$) showed some interesting features involving bubble motion. There were not many bubbles present at this speed and the rate of air ingestion was quite small. The movie showed that a group of bubbles immediately following

the interface in the groove was rotating counterclockwise and another group of bubbles, immediately adjacent to and following the first group, was rotating in a clockwise direction as sketched in Figure 6. There were no other bubbles present immediately behind this second group and therefore no method of visualization available to determine how many such vortices were present. Further from the interface and also in the grooves were bubbles moving along the leading edge of the groove toward the interface. Bubbles along the trailing edge of the groove were seen moving away from the interface in a film taken when the shaft speed was 350 rpm.

Another film, made when the shaft speed was 3360 rpm, shows a very turbulent interface with what appears to be ripples or waves in an air-water surface which were generally parallel to the bottom of the grooves. The gas ingestion rate was fairly high at this speed, but the flow in the vicinity of the interface was so complicated that no significant concept of the mechanism producing gas ingestion was gained from viewing the film.

Some exploratory experiments were conducted using a plain aluminum cylinder 3.990 inches in diameter installed inside the acrylic cylinder having an inside diameter of 4.002 inches. Alcohol-water solutions and glycerine-water solutions were used. The alcohol-water solutions with from about one to three per cent alcohol resulted in the most

severe gas ingestion observed with the alcohol-water solutions. The air-liquid mixture took on a foamy appearance for this range of compositions. With glycerine used in the annulus the interface appeared to remain stable and no gas ingestion was seen up to the maximum operating speed of 3600 rpm. With 50% glycerine, air ingestion was observed at about 2100 rpm. With a continued decrease in the proportion of glycerine used there was a decrease in the shaft speed at which gas ingestion was first seen.

The initial series of tests was completed on the viscoseal bearing described in reference (9). The pertinent dimensions of the bearing are as follows:

Diameter = 2.484"	Land width = 0.1667"
Radial clearance = 0.0025"	Groove width = 0.1667"
Overall length = 3.125"	Groove depth = 0.015"
Shaft diameter = 2.479"	$\alpha = 4.88^\circ$
Center supply groove width = 0.375"	$\beta = 7.0$
	$\gamma = 0.5$

The bearing, which was constructed with a central supply groove, had pumping lands of opposite hand pumping toward the supply groove. The bearing was made of brass and the shaft was made of Type 316 stainless steel.

The bearing film thickness was monitored with four Bently inductance probes. SAE 10 oil, which was used as the test fluid, was directed to the central supply groove through a flow control valve. The bearing was operated with a small leakage flow from each end. Thus, the supply

pressure was slightly larger than the head developed by the seal. The oil temperature was measured at the supply inlet and in the drain from each end of the bearing. The oil exit temperature was taken as the film temperature in the bearing and viscosities based on this temperature were used in the calculation of the bearing performance.

Figure 7 shows the eccentricity ratio, ϵ , plotted against the attitude angle, ϕ . These data were obtained for randomly selected loads, speeds, and oil supply pressures. It was noted that the bearing operated at high eccentricity ratios even when operated at low loads and high speeds. Further, it was observed that the eccentricity ratio was sensitive to the oil supply pressure.

Figure 8 shows a set of test points taken to study the scatter observed in the data in Figure 7. The data for Figure 8 were obtained at a constant load of 163.5 lb and a constant speed of 1275 rpm with various supply pressures. The numbers associated with the data points in Figure 8 refer to the supply pressure in psi. It will be noted that increasing supply pressure causes the eccentricity ratio and attitude angle to increase.

Figure 9 shows the experimental eccentricity ratio as a function of the capacity number C_n . The capacity number is defined as:

$$C_n = S_n \left(\frac{1}{d} \right)^2 = \frac{\mu N'}{P} \left(\frac{r}{c} \right)^2 \left(\frac{1}{d} \right)^2. \quad (4)$$

In this study "l" was taken equal to the land width in the bearing, there being 9 such lands in the viscoseal bearing. The theoretical curve is a plot of the equation,

$$C_n = \frac{(1 - \epsilon^2)^2}{\pi \epsilon} \left[\frac{1}{\pi^2 (1 - \epsilon^2) + 16 \epsilon^2} \right]^{1/2}, \quad (5)$$

known as the short bearing approximation (14).

From Figure 9 it will be noted that the short bearing approximation provides a reasonable estimate of the radial capacity for the particular viscoseal employed in this test. However, it is not clear that this approximation is satisfactory for all geometric parameters.

A study has been initiated to extend the work of Archibald and Hamrock (15,16) to the geometry of the viscoseal bearing. A numerical program is being developed for the IBM 360 to determine the load capacity and stability of the viscoseal geometry. This analysis considers the variation in film thickness over the lands and grooves due to eccentricity as well as the change due to the groove itself. The research participant on this project task has an independent source of support and does not receive a stipend from the NASA Grant NsG-587. The test facility and shop work will be provided from the grant.

The investigation of the buffered bushing seal continued through this period with effort on literature studies, analysis, and test equipment design.

Several papers have been published on the resistance of a flow through co-axial cylinders with a rotating inner cylinder. Suzuki (17) experimented with flow through short cylinders using large clearances and high Reynolds numbers. Cornish (18) measured the resistance of a flow through co-axial cylinders having fine clearances. Tomita (19) measured the resistance of a flow when the outer cylinder rotates. Recent work by Yamada (20) studies the resistance of a water flow through co-axial cylinders when the inner cylinder rotates. Yamada used large clearances and high Reynolds numbers.

However, none of the previously mentioned papers considered the effect of eccentricity on the axial flow rate and pressure drop using small clearances (i.e. $100 \leq r/c \leq 1000$) and high Reynolds numbers. It is difficult to determine whether or not Yamada's results are valid for small clearances and high Reynolds numbers.

The purpose of this research task is to investigate the effect of the following parameters on the pressure drop for a flow through an annulus formed by two co-axial cylinders with the inner cylinder rotating and the outer cylinder stationary:

- a) axial Reynolds number.
- b) rotating Reynolds number.
- c) clearance to radius ratio.
- d) eccentricity ratio.

e) surface roughness.

It is also planned to determine the entrance length for this type of flow as a function of the above parameters since most practical buffered seals will tend to have low L/D ratios. The apparatus will be operated primarily in the turbulent region of axial and rotating Reynolds numbers.

The experimental equipment for the testing of turbulent buffered bushing seals has been designed and is being constructed. It is anticipated that this apparatus will be in operation during the summer of 1968.

The test facility has been designed in such a manner that it may be modified to perform experimental work on viscoseals as well as research on gas-liquid buffer fluid mixtures.

V. PROPOSED SCHEDULE

During the period April 15, 1968 - October 15, 1968 the following efforts are scheduled:

1. Complete the experimental study of seals 3H and 6H.
2. Conduct additional tests of seals 11,12, and 13 using mixtures of glycerol and water in order to expand range of Re_c .
3. Determine the effect of back-flow on seal performance and air ingestion of seals 11,12, and 13.
4. Compare the pressure gradients obtained with fluid manometers with those obtained by using high frequency response instrumentation.

5. Complete the numerical computation of the load capacity and stability of the viscoseal bearing.
6. Complete the analysis and experimentation on the interface stability study and begin the report preparation.
7. Complete construction and assemble the buffered seal test rig.

REFERENCES CITED

1. Stair, W. K., "The Visco Seal - A Survey," Report ME 5-62-2, The University of Tennessee, March 1962.
2. Stair, W. K., "The Theoretical and Experimental Studies of Visco-Type Shaft Seals," Mechanical and Aerospace Engineering Research Report ME 64-587-1, University of Tennessee, October 23, 1964.
3. Stair, W. K., "Theoretical and Experimental Studies of Visco-Type Shaft Seals," Mechanical and Aerospace Engineering Research Report ME 65-587-3, University of Tennessee, May 21, 1965.
4. Stair, W. K., "Analysis of the Visco Seal - Part I, The Concentric Laminar Case," Mechanical and Aerospace Engineering Research Report ME-65-587-2, University of Tennessee, January 18, 1965.
5. Stair, W. K., R. H. Hale, "Analysis of the Visco Seal, Part II - The Concentric Turbulent Case," Mechanical and Aerospace Engineering Research Report ME 66-587-7, University of Tennessee, June 28, 1966.
6. Stair, W. K., "Theoretical and Experimental Studies of Visco-Type Shaft Seals," Mechanical and Aerospace Engineering Research Report, ME 66-587-5, University of Tennessee, April 28, 1966.
7. Stair, W. K., "Theoretical and Experimental Studies of Visco-Type and Buffered Shaft Seals," Mechanical and Aerospace Engineering Research Report ME 66-587-8, University of Tennessee, November 1966.
8. Stair, W. K., C. F. Fisher, Jr., "Theoretical and Experimental Studies of Visco-Type and Buffered Shaft Seals," Mechanical and Aerospace Engineering Research Report ME 67-587-9, University of Tennessee, May 1967.
9. Stair, W. K., C. F. Fisher, Jr., T. A. Arehart, Jr., "Theoretical and Experimental Studies of Visco-Type and Buffered Shaft Seals," Mechanical and Aerospace Engineering Research Report ME 67-587-10, University of Tennessee, October 1967.
10. Zuk, John, L. P. Ludwig, and R. L. Johnson, "Flow and Pressure Field Analysis of Parallel Groove Geometry for an Incompressible Fluid with Convective Inertia Effects," NASA TN D-3635, Washington, D. C., September 1966.

11. Saffman, P. G., G. Taylor, "The Penetration of a Fluid Into a Porous Medium or Hele-Shaw Cell Containing a More Viscous Liquid," Proceedings of The Royal Society, Series A, Vol. 245, 1958, 312.
12. Taylor, G., "The Instability of Liquid Surfaces When Accelerated in a Direction Perpendicular to Their Planes. I," Proceedings of The Royal Society, Series A, Vol. 201, 1950, 192.
13. Lewis, D. J., "The Instability of Liquid Surfaces When Accelerated in a Direction Perpendicular to Their Planes, II," Proceedings of The Royal Society, Series A, Vol. 202, 1950, 81.
14. Ocvirk, F. W., "Short Bearing Approximation for Full Journal Bearings," NACA TN 2808, Washington, D. C., October, 1952.
15. Archibald, F. R. and B. J. Hamrock, "The Rayleigh Step Bearing Applied to a Gas-Lubricated Journal of Finite Length," Journal of Lubrication Technology, Trans. ASME, Series F, vol. 89, No. 1, Jan. 1967, pp. 38-47.
16. Hamrock, B. J., "Rayleigh Step Journal Bearing: Part 1 - Compressible Fluid," Journal of Lubrication Technology, Trans. ASME, Series F, vol. 90, No. 1, Jan. 1968, pp. 271-280.
17. Suzuki, S., Jour. Fac. Eng., Imp. Univ. Tokyo, No. 18 (1929), p. 71.
18. Cornish, R. J., Proc. Roy. Soc. Lond., Ser. A. Vol. 140 (1933), p. 227
19. Tomita, K., Trans. Japan Soc. Mech. Engrs., Vol. 1, No. 5, 1935, p. 361.
20. Yamada, Y., Trans. Japan Soc. Mech. Engrs., Vol. 5, No. 18, 1962, p. 302.

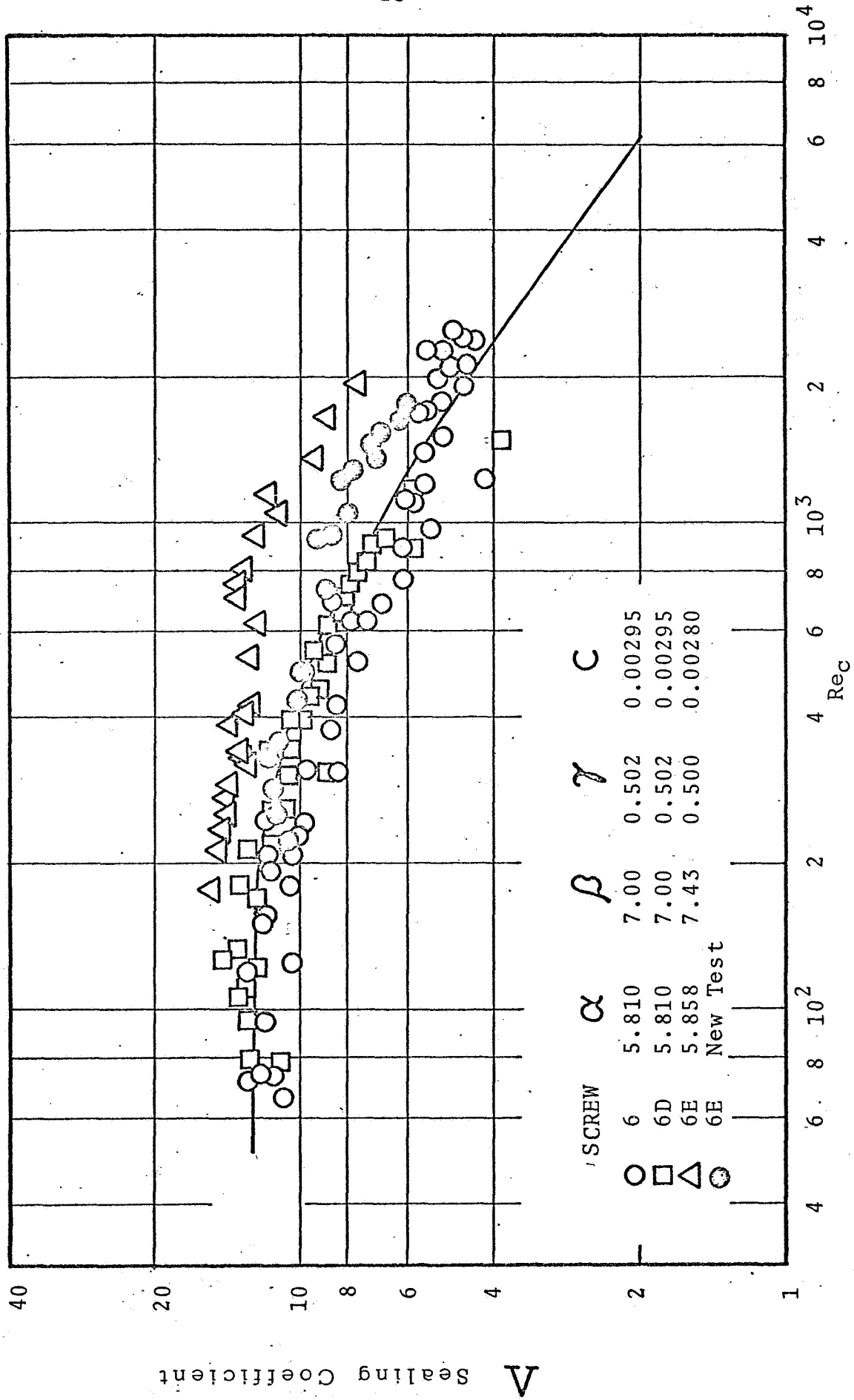


Figure 1. Theoretical and Experimental Sealing Coefficient for Seals 6, 6D, and 6E.

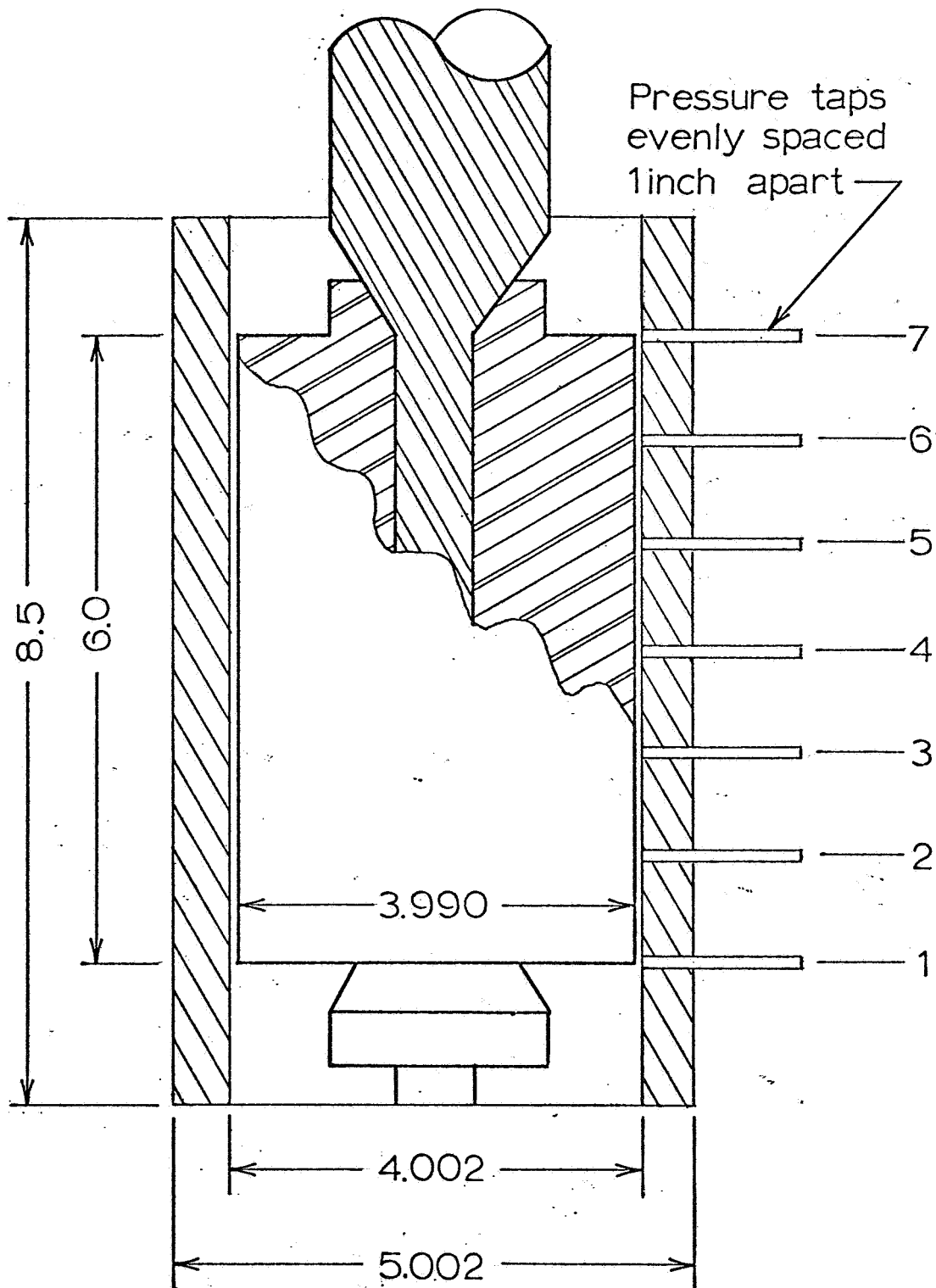


Figure 2. Test Arrangement for Seals 11, 12, and 13

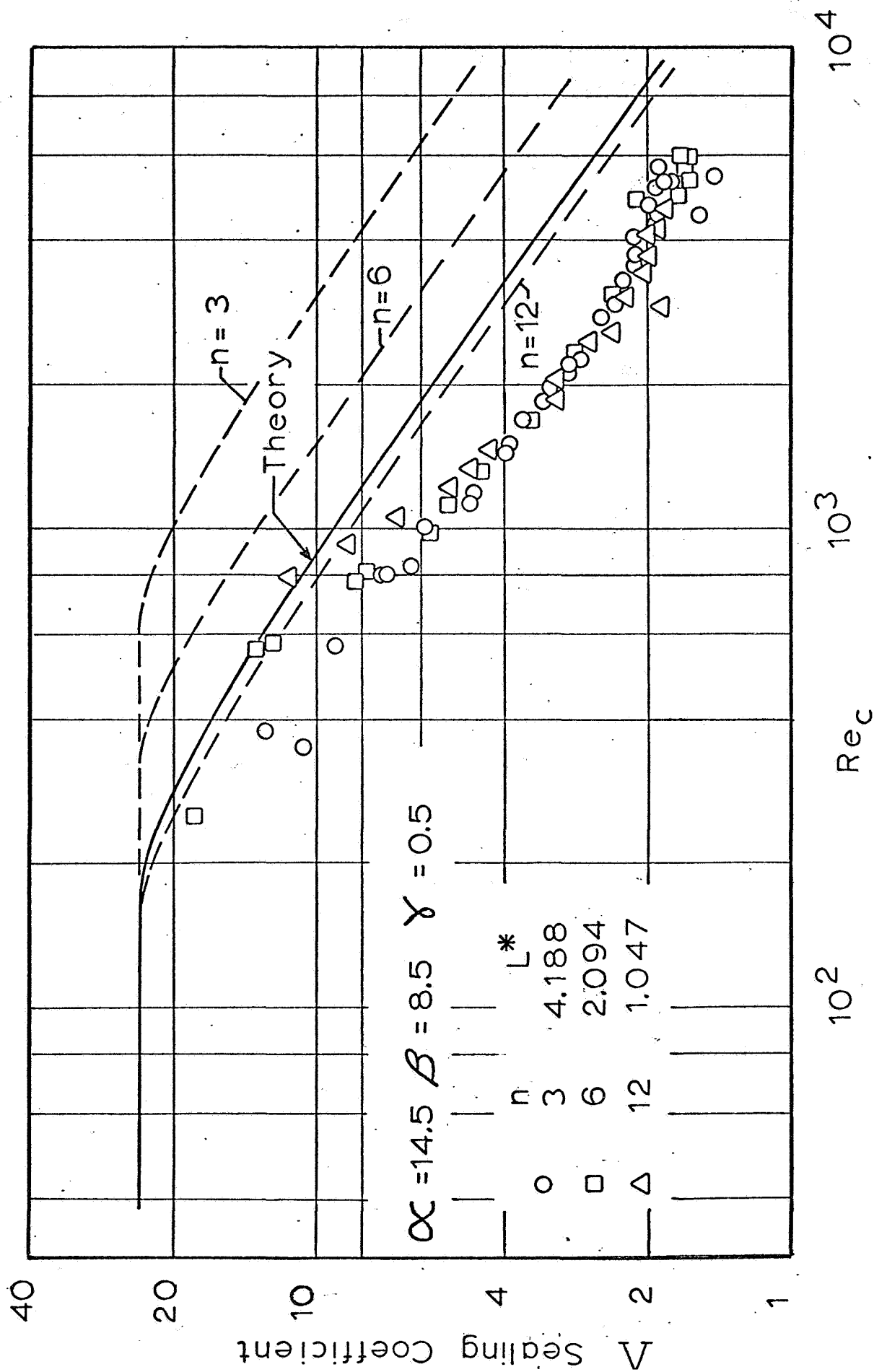


Figure 3. Theoretical and Experimental Sealing Coefficients for Seals 11, 12, and 13.

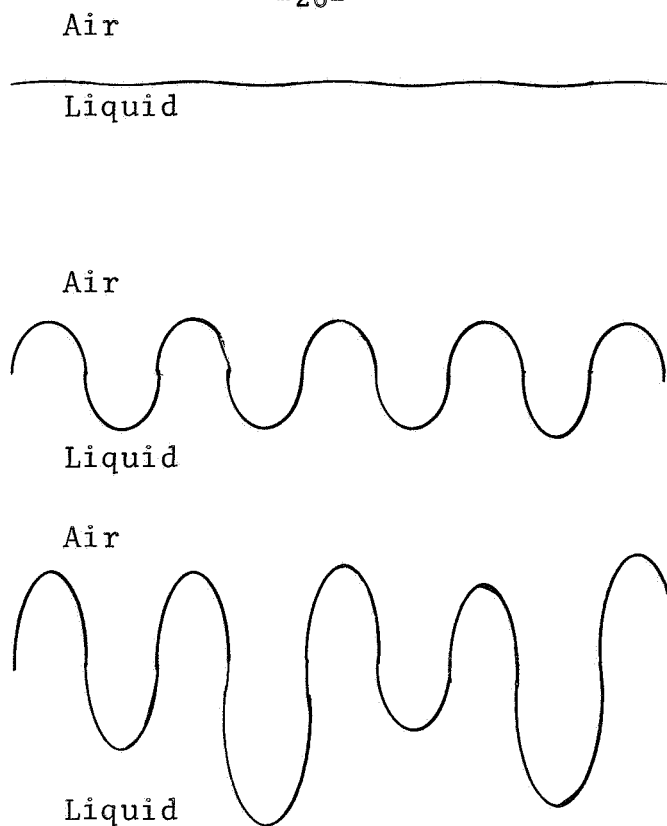


Figure 4. Progressive stages of growth of "fingers" of one fluid into another.

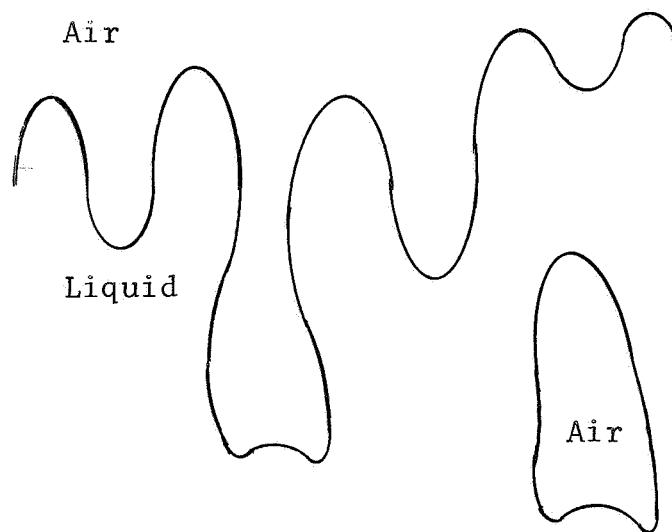


Figure 5. Sketch of possible development of interface configuration to cause entrapment of air bubbles in an annulus.

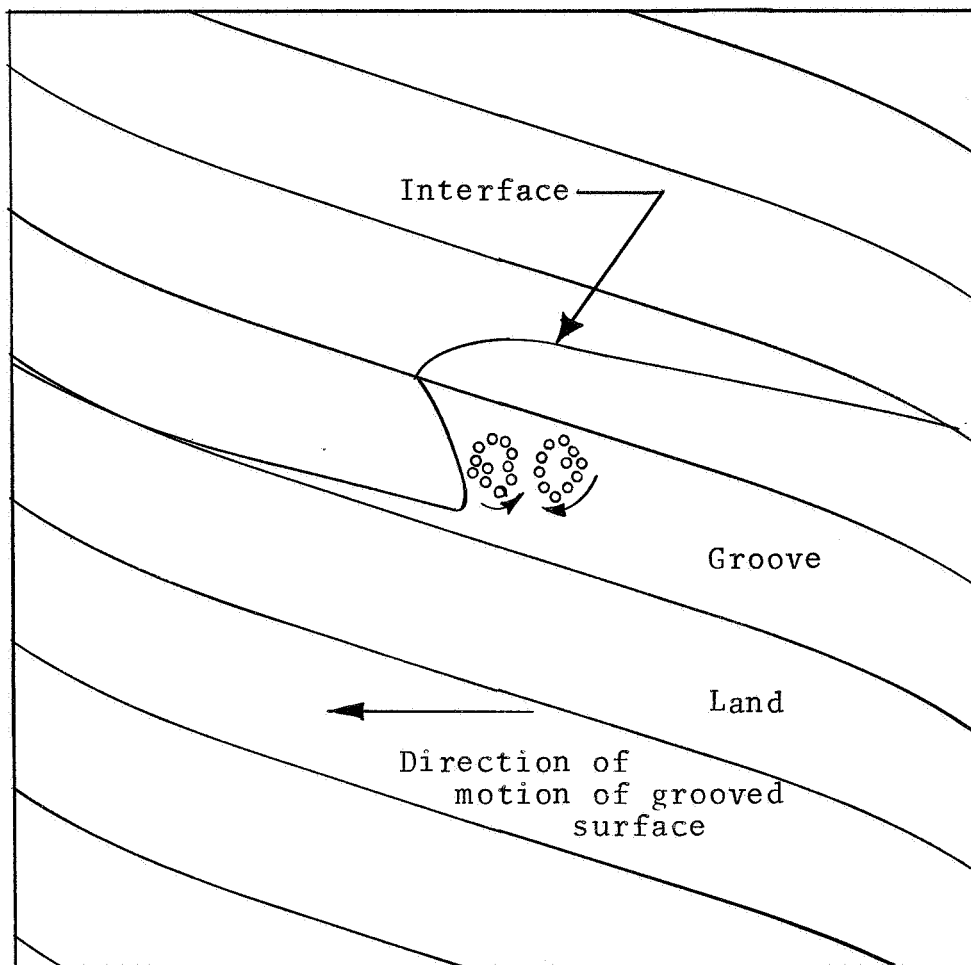
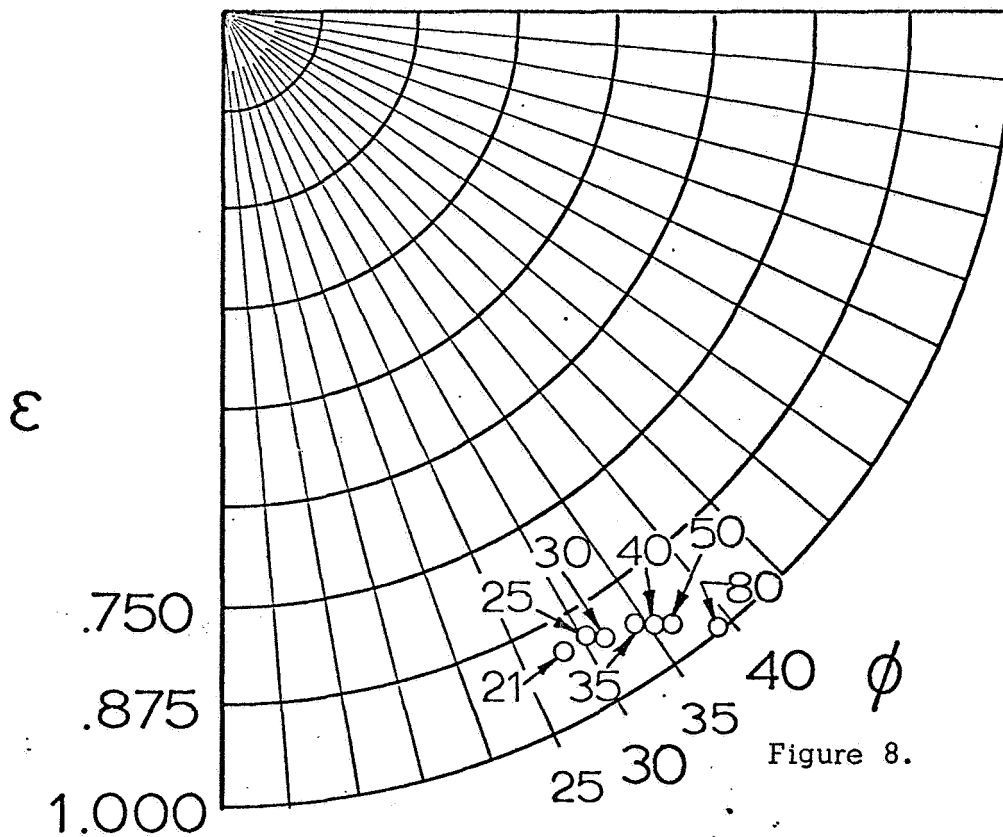
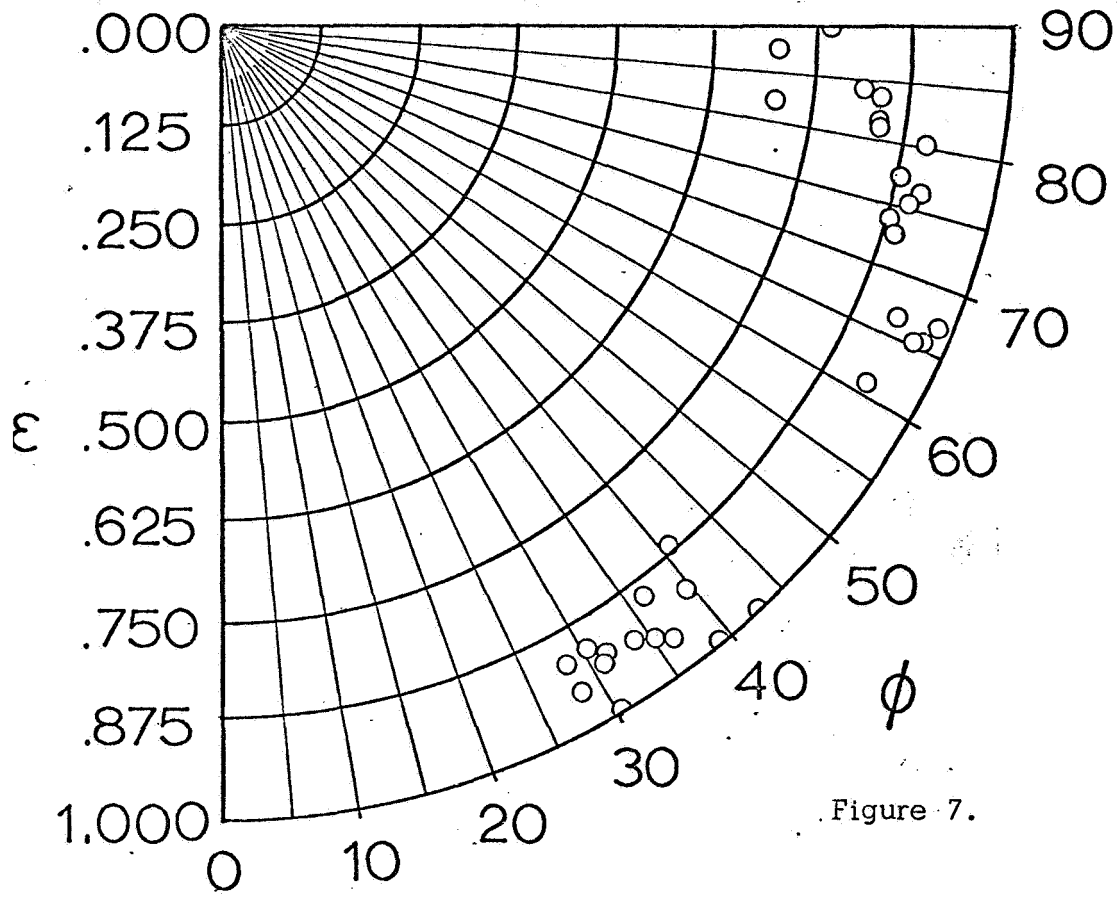


Figure 6. Sketch of air bubble motion in operation of viscoseal at 380 rpm.



Eccentricity Ratio versus Attitude Angle for Viscoseal Bearing.

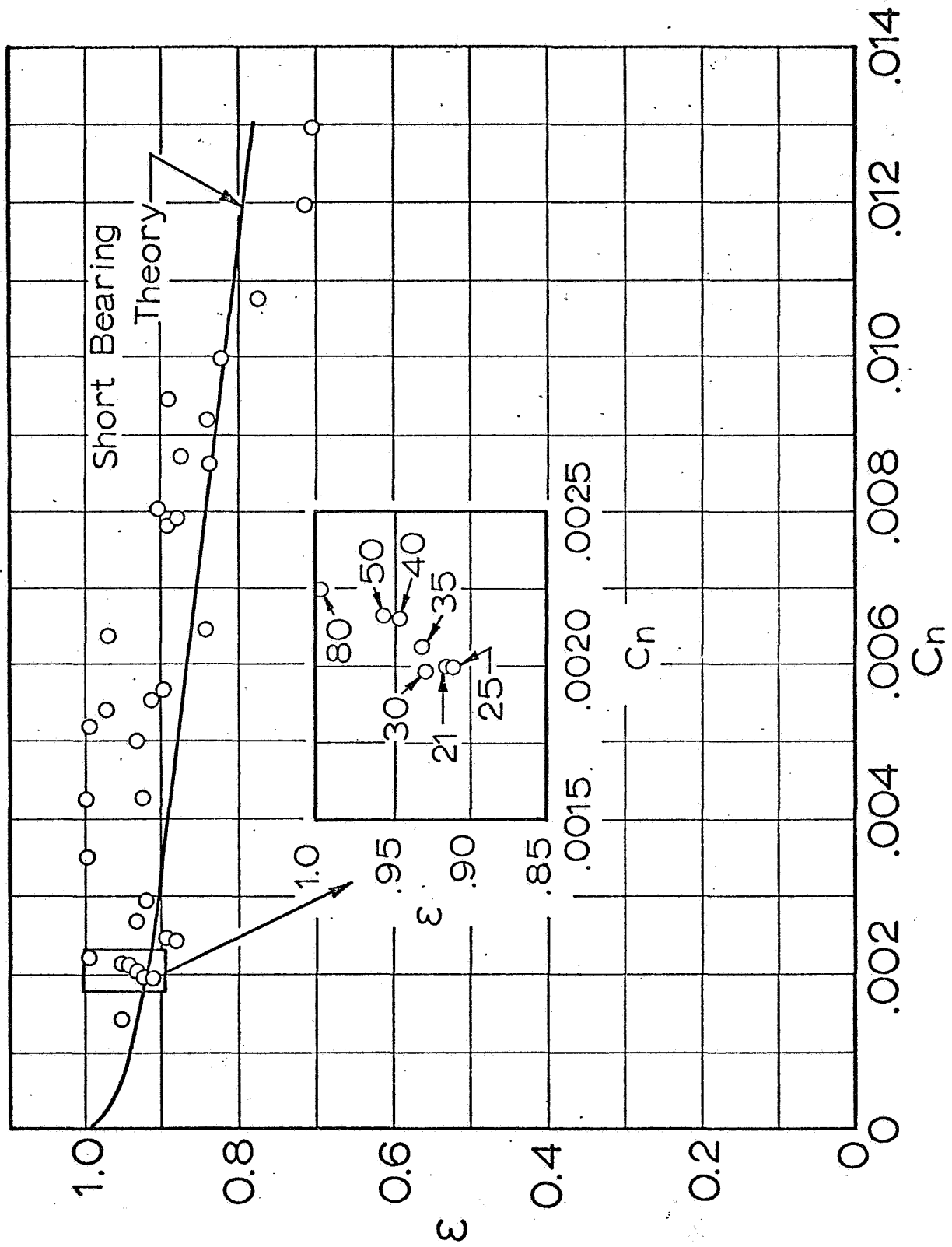


Figure 9. Eccentricity Ratio versus Capacity Number for Viscoseal Bearing.